18th International Conference
ENGINEERING MECHANICS 2012
Svratka, Czech Republic, May 14 – 17, 2012

pp. 1319–1329
Paper #288

FATIGUE UNDER FRETTING CONDITIONS

M. Španiel, M. Nesládek, J. Jurenka, J. Kuželka, J. Růžička*

Abstract: *Presented paper deals with application of phenomenological fatigue criteria on fatigue under fretting conditions. The objective is evaluation of fretting fatigue based on phenomenological criteria calibrated with relatively small set of experiments. Numerical stress analysis using finite element method was used (as usual in engineering applications) to determine stress fields and relative slips in contact interface of specimen in experimental set up. These quantities serve as input to several fatigue criteria that are to be compared each to other and evaluated. Optical measuring system DANTEC DYNAMICS Q-450 employing digital image correlation method for displacement field evaluation was used to calibrate and verify numerical model of friction. Basic results of experiments and computations are presented to be discussed.*

Keywords: ***Fatigue, fretting.***

1. Introduction

By definition, fretting fatigue is characterized as fatigue damage caused by stress peak concentrated near contact interface accelerated due to small relative tangential movements of contacting surfaces. Fretting fatigue occurs particularly in pressed joints, turbine blades lock joints, slot couplings and other typical machines parts. Stress field at the vicinity of contact interface, friction and partial slipping of contact surfaces are commonly considered as significant parameters affecting fretting fatigue.

1.1. Assumptions and classification of fretting

The values of relative slips of the contacting surfaces are widely used for description of the contact regimes under the fretting conditions Hoeppner (2006). Regarding the slip range, those regimes are: the *stick regime* with the slip magnitude up to $3\,\mu\mathrm{m}$, the partial slip regime with the slips from 3 to $50\,\mu\mathrm{m}$, and the gross sliding where the slips are more than $50\,\mu\mathrm{m}$.

It should be noted that the relation between the slip magnitudes and the fatigue life is not monotonic. One can observe a dramatic decrease in the partial slip regime. This state is specific for sticking in the centre of the interface and for slipping of both surfaces around the contact edges – see figure 1. This is the area of the most severe material damage which can, together with high stresses, act as "the weakest link" accelerating fatigue crack nucleation.

Decrease of the fatigue life in the partial-slip regime is followed by a rapid increase in the phase of transition to the gross sliding. This is due to intensive material erosion removing initial cracks. Note, that from practical point of view the exposed component will be damaged with abrasion instead of fatigue in such a case.

All the three above mentioned factors – stress, friction and contact slips – are closely dependent and in the real structures they change during their life-time.

1.2. Fretting fatigue evaluation approaches

Due to the multi-axial stress state in the fretted contact, conventional multi-axial fatigue criteria based on the critical plane estimation are widely used to predict the place of the initiation and the direction of the initial crack growth. Relations for conversion of some of these criteria to the number of cycles can be found e.g. in Navarro (2008). The target of presented research is to evaluate fatigue damage under

*Associate Prof. Ing. Miroslav Španiel, CSc., Ing. Martin Nesládek, Ing. Josef Jurenka, Ing. Jiří Kuželka, Ing. Jan Růžička
Faculty of Mechanical Engineerig, Czech Technical University in Prague, Technická 4; 166 07, Prague; CZ, e-mail: miroslav.spaniel@fs.cvut.cz

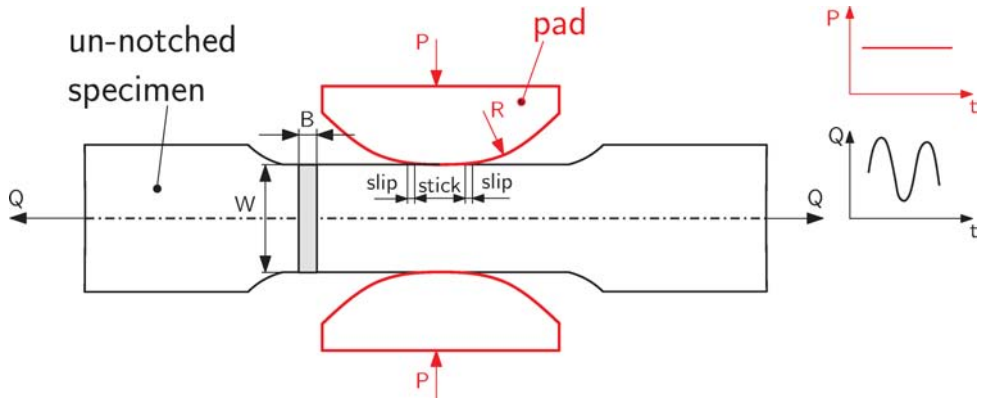

Fig. 1: A typical laboratory configuration for simulation of partial-slip fretting conditions (cylinder on a flat contact geometry)

fretting conditions. Evaluation is based on phenomenological criteria the verification of which should be based on reliable experimental and computational results. As mentioned, fretting is understood as fatigue process, therefore fatigue criteria are common base of fretting evaluation. Some authors have been trying to include surface wear simulation (based on the Archard's formula Madge (2007) or the dissipated energy concept Mary (2007)). Nevertheless, incremental estimation of wear together with damage cumulating is still infeasible for practical application on real structures.

Another possibility how to improve the results of conventional fatigue criteria is to incorporate certain correction with respect to the fretting wear. Ideally, it should reflect the values that cause surface damage, i.e. relative slips and surface shear stress. Ding et al. introduced a simple parameter correcting the multiaxial SWT criterion. According to the authors, the main contribution of it is that SWT can now handle the increase in the fatigue life in the transition domain between the partial and gross slips.

Evaluation of fatigue damage under fretting conditions based on phenomenological criteria is target of presented research. Verification of fretting fatigue criteria have to be based on reliable experimental and computational results. Quantities describing local material loading as stress field, contact slips etc., the measurement of which is very difficult, are in practice often calculated using finite element method. It is dependent on phenomenological description of friction. That is why we decided to verify and identify numerical model of experimental set up from the point of view of friction.

Material loading parameters as stress field, contact slips etc., the measurement of which is very difficult, are in practice usually calculated using finite element method. It is dependent on phenomenological description of friction. That is why we decided to verify and identify numerical model of experimental set up from the point of view of friction.

2. The experiments

Phenomenological modelling always requires experiments for both calibration and verification purposes. Therefore, experimental research represents important part of presented project. We have designed, manufactured and tuned up experimental set up utilizing electromagnetic pulsator AMSLER. Series of fatigue experiments under fretting conditions was carried out on the set up. Moreover the measurement of contact slips using digital image correlation optical method was implemented.

2.1. The experimental set up description

Original set up for testing of fatigue under fretting conditions developed in the scope of an acknowledged project was designed as a single dog-bone specimen in contact with two cylindrical pads causing fretting (see fig. 2). The main advantage of the cylinder on flat contact geometry is the possibility of its use in standard fatigue testing machines. The specimen is clamped in the jaws of the testing machine and loaded by a time-varying force in axial (vertical) direction. The loading frequency (as follows from the testing machine principles) corresponds to the natural frequency of the system which reflects the mass

Tab. 1: Loading conditions and number of cycles to crack initiation in the fretting experiments.

Experiment no.	Q_{amp} [kN]	Q_{mean} [kN]	P [kN]	N [cycles]
1	14	15	15	2 849 000
2	14	15	5	1 577 000
3	14	15	15	1 676 000

of the machine and the stiffness of additional experimental equipment and the specimen and reaches approximately 100 Hz. The normal contact force is kept approximately constant during a single test and acts in the horizontal direction which is perpendicular to the axial cyclic loading.

The material of the specimens was Cr-Ni-Mo-V martensitic steel with the plain fatigue strength in reversed tension $f_{-1} = 485\,\mathrm{Nmm}^{-2}$. The cross-sectional dimensions were thickness $B = 6\,\mathrm{mm}$ and width $W = 20\,\mathrm{mm}$ (see figure 1). Fretting pads with the radius $R = 200\,\mathrm{mm}$ were used.

After preliminary tests some modifications of experimental set up had to be done to eliminate weaknesses of experimental setup that manifested themselves through relatively high scatter of measured lifetime under assumed the same conditions (lading conditions and measured lifetimes estimation of which is based on the stiffness decrease in the experimental set up, can be found in table 1). Especially the difference between tests no. 1 and 3 reflects certain auxiliary influence. Fatigue crack initiation always took place on the top contact edge–see figures 3 that is vertically oriented according to the position of the specimen in the testing rig (figure 2). This fact is in agreement with the general observations. According to them crack occurs in the slipping area of a partial-slip regime contact. This is also the place of the most severe damage of the exterior faces as can be visually evaluated from the pictures of the surface relief. By contrast, mild damage of the central contact area where sticking occurs can be seen. Relief

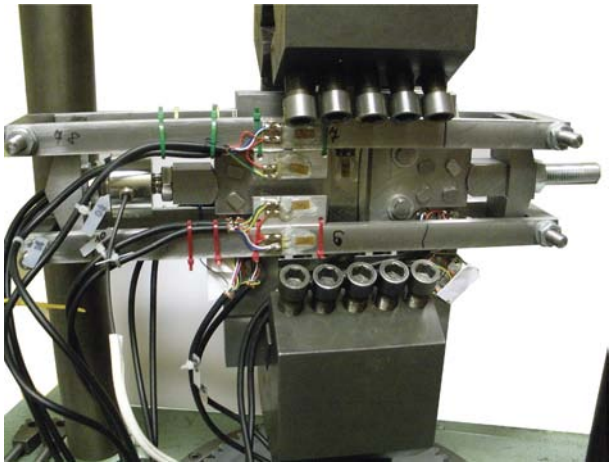

Fig. 2: The setup for the fretting fatigue testing. The equipment is clamped in the electromagnetic pulsator AMSLER.

of both contact surfaces of each specimen was scanned by a digital microscopic camera with 2Mpix resolution. Panoramic pictures, like those in figure2, were then obtained by merging more than 100 single scans. In some cases, the contact area was shifted from the centre of thickness towards the edge of the specimen, as shown at figure 3. This violates the uniform load distribution between both specimen edges assumption. Revision of the testing apparatus was done in order to reveal sources of this problem. Severe inaccuracy in the surface finish of the fretting pads was detected by roughness tester. In the thickness direction, the measured surface contour was curved, so more precise finishing was performed on a CNC machine. A detail of original pad installation is shown in figure 4. Rigidity of this design did not allow rotation of the fretting pads which could eliminate the initial non-parallel set up of the contact surfaces. That is the reason why additional chamfers were manufactured. Together with lateral gaps as shown in figure 5 this arrangement is capable of compensating the initial inaccuracies given by manufacturing.

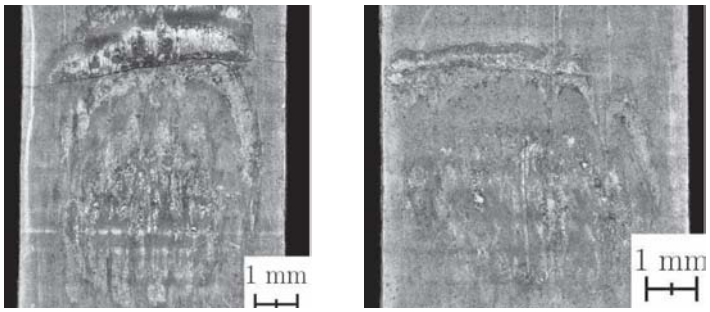

Fig. 3: Detail of worn contact surfaces of the specimen after fretting test no. 1

Fig. 4: Detail of the fretting pad installation in the experimental equipment – the original configuration without chamfers.

Usually no fatigue cracks occur on the pads after the experiment termination. The contact surfaces can then be renovated by grinding and after that the pads can be reused. Since this is a costly operation, the following simple modification of the fretting pad installation was introduced. Both pads are now fixed in a moderately rotated position (compare figure 5 and figure 6). Due to this, the contact area is shifted horizontally on the fretting pads which enable their one-off reuse when they are installed upside down. The beneficial effect is that it will halve the time losses and expenses for their renovation.

3. Experimental results

31 relevant experiments with specimens made of creep-resistant chromium steel were carried out at the Czech Technical University in Prague.

The loading conditions–axial prestress Q_{mean} and amplitude Q_{amp} as well as pressing force P, numbers of cycles to detected crack N and number of cycles N_{corr} renormalized to $1\,\mathrm{mm}$ crack[**] for the experiments are presented in Table 2. Note that experimental observations proved that the initiation phase represents the major part of specimen lifetime. Long crack growth period is negligible. Thus the achievement of $1\,\mathrm{mm}$ crack length can be satisfactorily considered as the initiation.

Four levels of periodical axial load Q and two levels of constant pressure force P were tested. Axial loading frequency was about $120\,\mathrm{Hz}$.

Averaged Wohler curve under fretting conditions in comparison with plain fatigue one is plotted in figure 6. All measured data were used together to determine linear dependency of axial stress amplitude

[**] Renormalized lifetime was computed by extrapolation of subsequenly measured crack growth data for most of specimens.

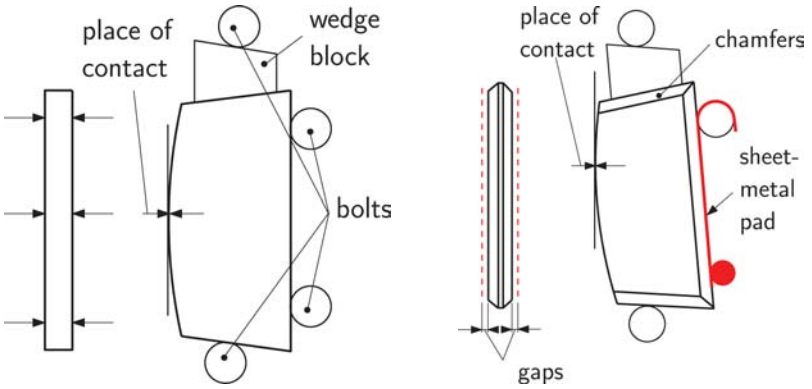

Fig. 5: The original (left) and modified (right) fretting pad geometry with flat side faces. The rotated position enables reusing of the same pad.

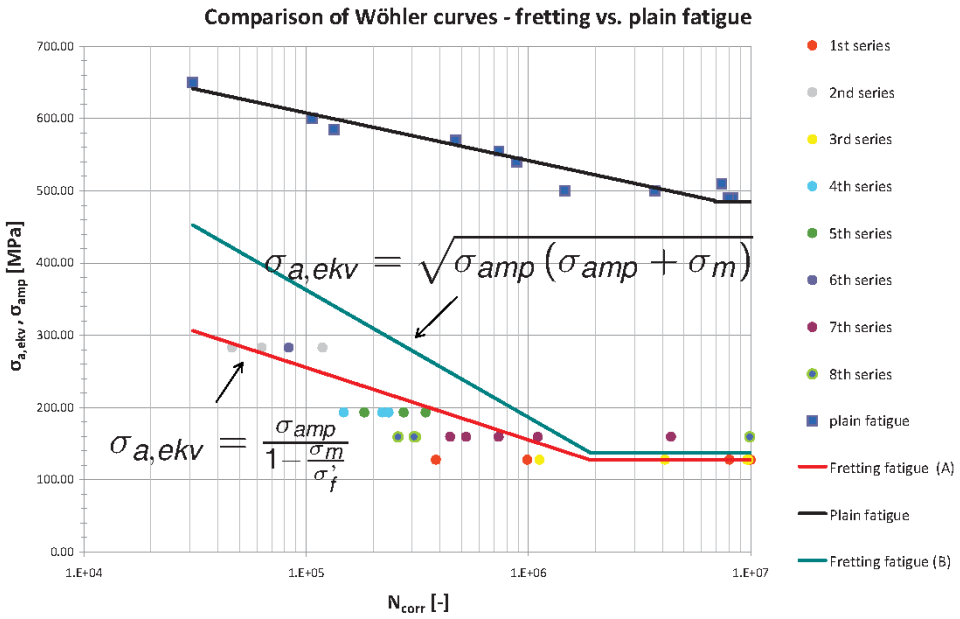

Fig. 6: Comparison of plain fatigue and fretting fatigue Wohler curves. The colours correspond with table 2.

σ_{amp} (of real loading cycle) on number of cycles N_{corr} causing crack initiation. Then the curve was recomputed with respect to amplitude $\sigma_{a,ekv}$ of equivalent alternating loading cycle (according to two commonly used formulas shown directly in figure 6) and plotted together with plain fatigue curve.

Tab. 2: Complete list of fretting fatigue tests.

Spec.	Q_{amp} [kN]	Q_{mean} [kN]	P [kN]	N [-]	l_0 [mm]	N_{corr} [mm]
1	14	15	5	500000	1.5	-
2	14	15	5	-	-	-
3	14	15	5	10 000 000	No init	10 000 000
17	14	15	5	1 160 000	2.40	987 700
23	14	15	5	260 000	0.33	383 600
25	14	15	5	8 180 000	2.20	8 024 000
26	14	15	5	10 000 000	No init	10 000 000
27	14	15	5	10 000 000	No init	10 000 000
4	28.1	30.1	5	126 500	4.10	118 300
5	28.1	30.1	5	70 000	3.20	63 100
6	28.1	30.1	5	40 000	0.40	46 430
7	14	15	15	9 800 000	1.10	9 784 000
20	14	15	15	9 875 000	4.30	9 635 000
21	14	15	15	9 730 000	1.55	9 648 000
22	14	15	15	1 250 000	1.95	1 122 000
24	14	15	15	4 030 000	0.50	4 118 000
8	20.3	21.7	5	174 000	2.50	147 700
9	20.3	21.7	5	210 000	0.70	219 900
10	20.3	21.7	5	235 000	1.00	235 000
11	20.3	21.7	15	190 000	1.30	182 600
12	20.3	21.7	15	370 000	2.40	344 700
13	20.3	21.7	15	265 000	0.70	274 400
14	28.1	30.1	15	80 000	0.60	83 530
15	17.1	18.4	15	260 000	1.00	260 0000
16	17.1	18.4	15	4 447 000	2.80	4 380 000
18	17.1	18.4	15	450 000	1.10	444 200
19	17.	18.4	15	810 000	2.93/3.60	735 300
32	17.1	18.4	15	1 180 000	3.60	1 102 000
33	17.1	18.4	15	535 000	1.20	523 700
28	17.1	18.4	5	310 000	1,00	310 000
29	17.1	18.4	5	285 000	0.70	306 000
30	17.1	18.4	5	9 980 000	3.60	9 900 000
31	17.1	18.4	5	225 000	0.53	259 000

4. Calibration of friction model

The calibration is based on measurements of relative contact slips and their comparison with slips obtained from FE simulation. Simple Coulomb's friction model with the only parameter–friction coefficient μ– has recently been calibrated. Calibration itself is based on comparison between measured and calculated relative slip Δ along appropriate path near contact surface (see dot lines in figure 7). Calculations were done for various values of friction coefficient ($\mu \in \langle 0.1;\, 0.8 \rangle$) and the $\mu = 0.6$ representing the best agreement between measured and computed curve $\Delta\,(y)$ was determined as correct value for subsequent (fretting fatigue) calculations. To calibrate friction coefficient on the base of agreement of measured and

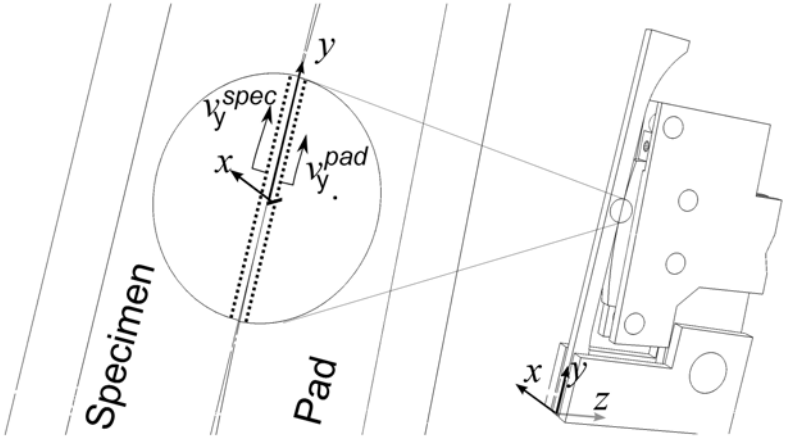

Fig. 7: Accumulated contact slips.

calculated response proper quantity for comparison of the experimental and numerical results must be chosen. The choice of the slip amplitudes along the contact area was found misleading for this purpose. According to the experimental results, this quantity is not convenient since approaching the bottom edge of the contact the slipping process becomes more stochasti (see figure 8). When using more averaged quantity better conformity can be expected. Accumulated slip per period of exciting axial load Q

$$\Delta\,(y) = \frac{1}{n}\int_{t_0}^{t_0+nT} \left| v_y^{spec}\,(y) - v_y^{pad}\,(y) \right| \mathrm{d}t\ , \tag{1}$$

seems to be a more suitable measure. This quantity has more understandable physical meaning than the slip amplitudes (in sense of dissipated work) and can be evaluated from both experimentally and computationally determined motion of surface points in the vicinity of contact. In equation (1) $T\,[\mathrm{s}]$ is the period of exciting force Q, n means number of periods of integration, $v_y^{spec}\,(y)$, resp. $v_y^{pad}\,(y)\ \left[\mathrm{mms}^{-1}\right]$ represents $y-\mathrm{component}$ of velocity of point with coordinate y along the contact edge[***]. Experimentally and computationally determined accumulated contact slips in dependence on the position in contact area after calibration procedure are plotted in graph on figure 9.

4.1. The measurements of relative slips

Dantec Dynamics Q-450 optical system was used for relative displacements measurements. Since displacements in order of $\mu\mathrm{m}$ had been measured at high frame rate, the demands on pattern quality and lighting were quite high. Regarding $1\,\mathrm{Mpix}$ resolution of CCD chip the objective and extension tubes were used to achieve spatial resolution of approximately $8\,\mu\mathrm{m/pix}$ with the field of view of about $\times 8\,\mathrm{mm}$. The viewed surfaces were clothed in a very fine contrast stochastic speckle pattern considering the recommendations in Kuželka (2010). Two special high frequency $1\,\mathrm{kW}$ lamps were used for sufficient lighting. The images of the vicinity of the contact interface between the specimen and pad were recorded by a high speed NanoSense Mk III camera with the frequency of 2 kHz (corresponds to

[***]The intersection of (common) contact surface with front surface of specimen (parallel with yz plane)laying on specimen, resp. pad in the vicinity of contact.

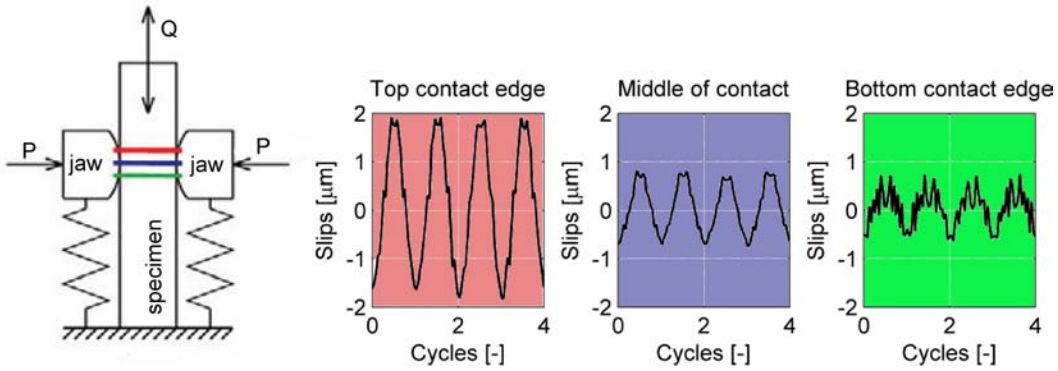

Fig. 8: Experimentally measured time history of relative slips in different locations in the contact interface for 10 kN *pressure loading.*

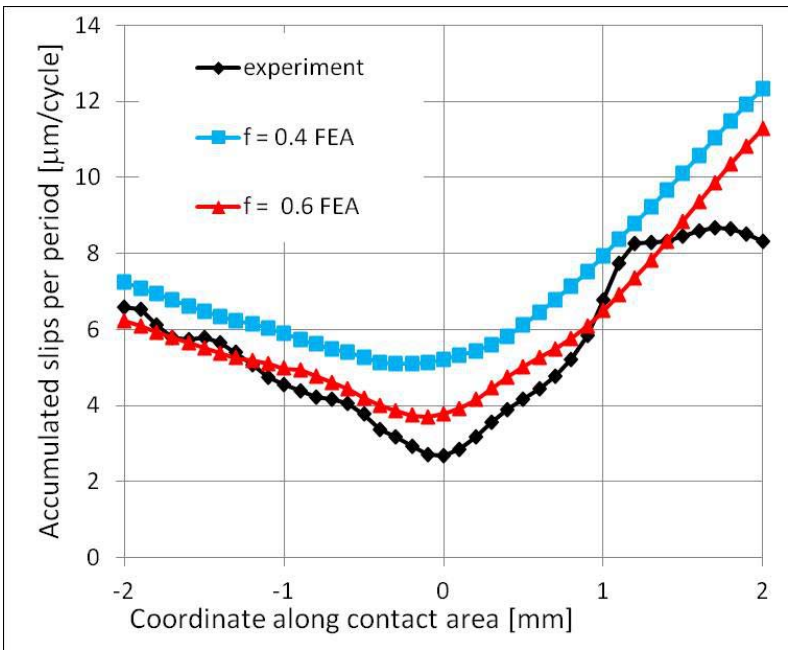

Fig. 9: Accumulated relative slips per single cycle period along the contact interface for 10 kN *pressure force* P*. Comparison of experimental and numerical results.*

20 images per loading cycle).Data were acquired during a relatively short period (about 50 cycles) after every 200 000 cycles. The acquired sets of image sequences were processed in the commercial image correlation software Istra 4-D. The displacements were evaluated in a $0.1\,\mathrm{mm}$ (12 pix) equally spaced grid. Each grid point corresponds to a subset $0.2 \times 0.2\,\mathrm{mm}$ (25×25 pix). The obtained results were further post-processed by Matlab scripts. The centre point of contact area was approximately located on the basis of horizontal displacement field in case of pure pressure loading of $P = 10\,\mathrm{kN}$. At this point, a coordinate system for relative slip evaluation was introduced (figure 10).

4.2. Calibrating of friction coefficient

To obtain required input data for the fatigue criteria, a 3D FE model of the testing apparatus was assembled – see figure 9 – and analysed. FE solver Abaqus was used for the numerical simulation which was divided into several computation steps reflecting pressure and axial pre load (static) and application of axial cyclic loading.(explicit dynamics). Plasticity of material was included as well. Geometry was discretized with linear hexahedron continuum elements. Smallest element edge in the contact area was approximately $85\,\mu\mathrm{m}$–see figure 11. A proper modelling of the contact friction has a significant effect on relative slips determination. Contact slips is the significant parameter of fretting fatigue evaluation.

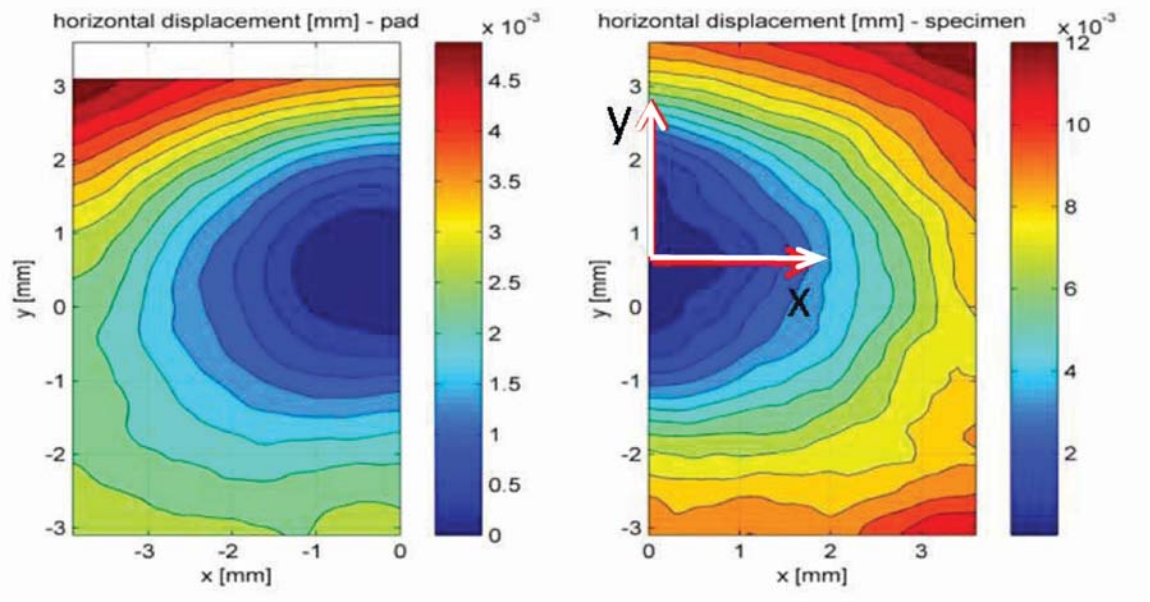

Fig. 10: Determining of contact center based on horizontal displacemet.

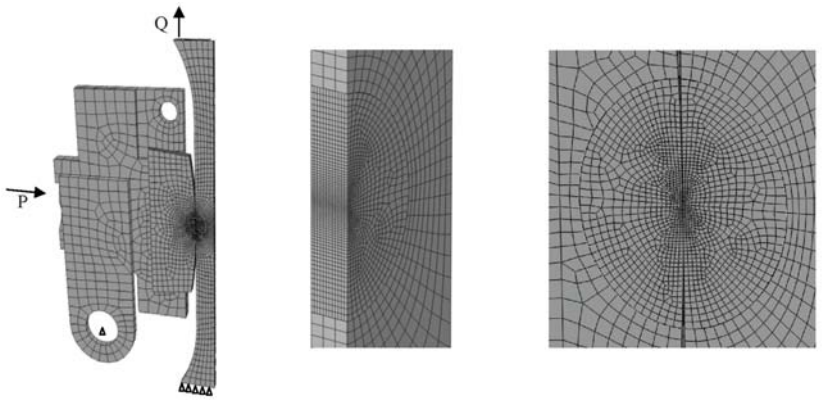

Fig. 11: FE model utilized for friction calibration. Detail of specimen mesh. Detail of contact area.

The friction coefficient used in the fretting simulations is usually higher than in a conventional contact and should reflect its change during the life-time. FE solver Abaqus contact algorithms adopt several computation techniques. In our model, surface-to-surface discretization, finite-sliding tracking approach and hard contact with the Coulomb friction was applied.

5. First results of fatigue analysis

Various multi-axial fatigue criteria were employed to evaluate experimentally measured fretting fatigue based on plain fatigue parameters of specimen material. Fatigue index approach has been utilized so far. Most of known multi-axial criteria used to evaluate high-cycle fatigue (HCF) can be written in form

$$\text{L.H.S} = af\left(C\right) + bg\left(N\right) \leq \text{R.H.S}\,, \tag{2}$$

where $f\left(C\right)$, resp. $g\left(N\right)$ are functions of shear C, resp. normal N stress amplitude, expressed from stress/strain invariants or from stress/strain components in some plane. These invariants or components were as usual calculated using finite element method. FE model was similar as model used for friction coefficient calibration. Constants a and b as well as right hand side R.H.S. of equation 2 representing

fatigue limit are material parameters. *Fatigue index* is defined as coefficient

$$\mathrm{FI} = \left(\frac{\mathrm{L.H.S.}}{\mathrm{R.H.S.}} \right) , \tag{3}$$

expressing material loading with respect to fatigue limit. To compare various criteria, fatigue index error

$$\Delta\mathrm{FI} = \left(\frac{\mathrm{L.H.S.} - \mathrm{R.H.S.}}{\mathrm{R.H.S.}} \right) \cdot 100\% = (\mathrm{FI} - 1) \cdot 100\% \tag{4}$$

was evaluated in small domains in vicinity of contact for loading representing experimentally determined

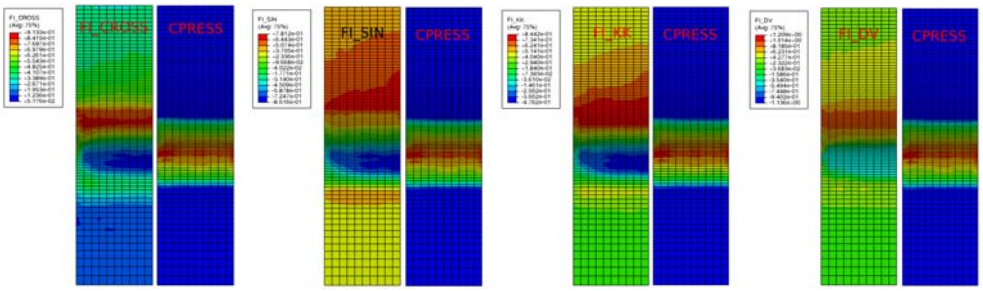

Fig. 12: Fatigue index FI *(left) and contact pressure* p *(right figure in pair) distribution at the vicinity of contacting surface. Four pairs from left to right represent Crossland, Sines, Kakun-Kawada and Dang Van criteria.*

fatigue limit (according to the graph on figure 9 $Q_{mean} = 15\,\mathrm{kN}$, $Q_{amp} = 14\,\mathrm{kN}$, and $P = 5\,\mathrm{kN}$ or $P = 15\,\mathrm{kN}$) for set of criteria including Crossland (Cross), Sines (Sin), Kakun-Kawada (KK), Dang Van (DV), Gonçalves, Araújo, Mamiya (GAM), Mamiya (Mam), Papuga (PCr). These criteria are well described in Papuga (2011). Fatigue index errors for these criteria are printed in table 3, examples of fatigue index along contact surface can be found in figure 12.

Tab. 3: Fatigue index error values for the selected multiaxial criteria.

	Fatigue index error ΔFI [%]						
P [kN]	Cross	Sin	DV	KK	GAM	Mam	PCr
5	2.1	-35.4	6.8	-6.8	14.9	12.7	14.8
15	25.1	-8.3	21.8	19.4	57.7	54.0	27.2

6. Conclusions

Series of 31 test simulating fretting fatigue conditions was done using flat dog bone samples from heat resisting chromium steel. Based on S-N curves of fretting tests and plain fatigue tests comparison (see figure 9) significant negative effect of fretting on lifetime of samples can be observed. Compared to the fatigue of smooth specimens in tension-compression alternating load fatigue limit decreased to the quarter of original value, i.e. $125\,\mathrm{MPa}$ for 3×10^6 cycles. No significant influence of various transversal pressure load of contact pads by values of $5\,\mathrm{kN}$ and $15\,\mathrm{kN}$ on life of samples could be seen. According to the nature of contact surfaces damage under different pressure loads different damaging micro mechanisms can be supposed as discussed bellow.

Significant variance of number of cycles to crack initiation for different specimens with the same loading probably follows from

- Non uniformly distributed contact pressure

- Initial surface roughness with possible surface defects from machining
- Other factors, especially boundary conditions

The closer the load approaches fatigue limit, the more significant variance appear. The higher load the lower variances. In all cases the location of crack initiation was the domain in upper part of contact.

Measured S-N curves served as base of verification of the ability of various HCF multi-axial criteria to predict fatigue failure under fretting conditions. Stress fields analysed by FEM were used as input into these fatigue criteria. Fatigue index error was used as measure of criteria quality. This research resulted into some hints and hypotheses:

1. Elastic-plastic material model in FE calculations provides us with much better fretting fatigue predictions, however elastic material model in FE analysis has negligible influence onto predicted crack placement
2. The best correspondence can be seen for Crossland and Dang Van criteria. For pressing force $P = 5\,\mathrm{kN}$ fatigue index error approaches almost zero. For $15\,\mathrm{kN}$ it is conservative. This tendency have shown all tested criteria.
3. All tested criteria except the Sines one are conservative. That is why the Sines criterion cannot be recommended.
4. Tested criteria do not evaluate the influence of pressing force correctly. While the experiments have not shown any difference in the life of flat dog bone specimens under pressing force $P = 5\,\mathrm{kN}$ and $P = 15\,\mathrm{kN}$, the criteria have. According to fractographic analysis, pressing load $P = 5\,\mathrm{kN}$ leads to more uniform damage of entire contact area. Probably some micro-nothes with high stress are formed. Conventional numerical models are not able to calculate these stresses. Surface areal damage under $P = 15\,\mathrm{kN}$ is much less, contact interface rather acts as a notch increasing the stress concentration at a point. It would be appropriate to consider some correction of criteria based on correlation of life and contact slips. Establish a reliable correction would require a further series of experiments with different pressing forces.

Acknowledgments

This project is kindly supported by GAČR grant no. 101/09/1709.

References

Hoeppner, D.W. (2006), Fretting fatigue case studies of engineering components. *Tribology Int.*, Vol. 39(10), pp. 1271–1276.

Papuga J. (2011), A survey on evaluating the fatigue limit under multiaxial loading. *Int J Fatigue*, Vol.33(2), pp. 153–165.

Vingsbo O., Soderberg, S. (1988), On fretting wears, *Wear*, Vol. 126, pp. 131-147.

Navarro, C., Mun?oz, S., Domínguez, J. (2008), On the use of multiaxial fatigue citeria for fretting fatigue life assesment, *Int. J. of Fatigue*, Vol. 30, pp. 32-44 .

Madge, J.J., Leen, S.B., McColl, I.R., Shipway, P.H. (2007), Contact-evolution based prediction of fretting fatigue life: Effect of slip amplitude,*Wear*, Vol. 262, pp. 1159-1170.

Mary, C., Fouvry, S. (2007), Numerical prediction of fretting contact durability using energy wear approach: Optimisation of finite-element model,*Wear*, Vol. 263, pp. 444-450

Ding, J., Houghton, D., Williams, E.J., Leen, S.B. (2011), Simple parameters to predict effect of surface damage on fretting fatigue,*Int. J. of Fatigue*, Vol. 33, pp. 332-342.

Kuželka, J., Chlup, H., Jurenka, J., Španiel, M. (2010), Fatigue degradation in the vicinity of contact interface under fretting conditions. In: *Proc. of Experimental Stress Analysis*, pp. 201-208. ISBN 978-80-244-2533-7.

Sutton A.M., Orteu J. and Schreier W.H. (2009), *Image Correlation for Shape, Motion and Deformation Measurements*Springer, New York.